Nickel- and Cobalt-Dependent Reagents Identify Structural Features of RNA That Are Not Detected by Dimethyl Sulfate or RNase T1†

Ping Zheng,‡ Cynthia J. Burrows,§ and Steven E. Rokita*,‡

Department of Chemistry and Biochemistry, University of Maryland, College Park, Maryland 20742, and Department of Chemistry, University of Utah, Salt Lake City, Utah 84112

Received October 7, 1997; Revised Manuscript Received December 16, 1997

ABSTRACT: Ribosomal 5S RNA presents a particular challenge to structural investigations since this polynucleotide is too large for complete NMR characterization but lacks significant tertiary structure to modulate, for example, diagnostic alkylation of guanine N7 by dimethyl sulfate. Nickel- and cobalt-dependent reagents that are sensitive to the N7 and aromatic face of guanine have now been applied to 5S rRNA (*Xenopus lavis*) and provide structural information that was not previously available from traditional chemical or enzymatic probes. Although G75 had repeatedly demonstrated an average reactivity with dimethyl sulfate and minimal reactivity with RNase T1, this residue was the major target of both metal-dependent reagents. Such reactivity provides crucial support for a structural model of loop E identified by prior physical, but not chemical, methods. Similarly, the tetraloop structure of loop D was more accurately reflected by the reactivity of G87 and G89 in the presence of the nickel reagent rather than in the presence of RNase T1. In addition, nickel-dependent modification of guanine residues surrounding the three-helix junction of loop A suggests an organization that is less compact than previously considered.

Numerous physical, chemical, and genetic methods are now routinely available for investigating problems in RNA structure and folding, and yet conformational analysis remains a significant challenge. As noted 5 years ago, ribosomal 5S RNA had been subjected to every imaginable technique without yielding a thorough description of its structure (*1*). A variety of new approaches have subsequently been developed and have continued to enrich our understanding of this RNA (*2*−*4*). Considerable effort has focused on 5S rRNA since it is an essential component of ribosomes and appears to interact with additional rRNA and a number of ribosomal proteins (*5*−*7*) as well as a transcription factor TFIIIa (*8*, *9*). This RNA is also an attractive model system for exploring fundamental issues of RNA conformation and RNA−protein interaction due to its relatively small size (∼120 nt) and rich array of noncanonical base pairs (*10*, *11*). These features were similarly appealing for study with two metal-dependent reagents, NiCR[1] and $CoCl_2$, that we have developed as reliable probes of guanine structure.

The sequence of 5S rRNA is highly conserved throughout nature, and phylogenetic analysis alone provided an initial model for its secondary structure (*12*). This model was later refined to include five helical regions, three internal loops, and two hairpin loops forming a Y-structure (*13*) and was quite similar to the current model illustrated in Discussion. Although tertiary interactions had previously been suggested by certain chemical, enzymatic, and spectroscopic data (*2*, *14*−*17*), a number of mutagenesis and chemical studies have since confirmed the absence of any long-range association (*3*, *18*, *19*). Our current understanding of 5S rRNA structure now derives from extensive application of chemical and enzymatic probes (*20*−*22*), computational methods (*10*, *23*), and NMR spectroscopy (*1*, *11*). In addition, a nuclease-resistant fragment of 5S rRNA from *Escherichia coli* has recently been elucidated by crystallography (*24*). However, many questions on conformation and dynamics persist. For example, prior data on the reactivity of loop E (see below) indicated two possible base-pairing and stacking arrangements (*20*, *21*), and later analysis by NMR offered yet a third alternative (*11*). Also, a more complete representation of loop A is needed to help define the flexibility and orientation of the three arms of 5S rRNA (*25*−*27*).

Guanine performs a key role in nucleic acid folding due to its capacity to form numerous hydrogen bonds and stacking interactions (*28*, *29*). This in turn necessitates the use of multiple reagents to probe the accessibility of various functional regions of this residue (*30*, *31*). Secondary or tertiary structure involving guanine N1, O6, and N7 can be identified by a characteristic resistance to strand cleavage by RNase T1 (*32*). Guanine N7 can also be examined by reaction with DEPC even though the predominant target of this reagent is adenine N7 (*33*, *34*). Typically, tertiary structure surrounding guanine N7 is identified by inhibition of N7 methylation by DMS. Secondary structure does not affect this methylation, and consequently DMS provides no information on the helical conformation of guanine N7 (*30*).

† This research was supported by the National Institutes of Health (GM-47531).

* Author to whom correspondence should be addressed.

‡ University of Maryland.

§ University of Utah.

[1] Abbreviations: DEPC, diethyl pyrocarbonate; DMS, dimethyl sulfate; NiCR, [2,12-dimethyl-3,7,11,17-tetraazabicyclo[11.3.1]heptadeca-1(17),2,11,13,15-pentaenato]nickel(II) perchlorate; Xlo, *Xenopus lavis* oocyte.

S0006-2960(97)02480-X CCC: $15.00
Published on Web 02/06/1998

In contrast, NiCR and $CoCl_2$ can provide significant results on both secondary and tertiary interactions of the N7 and aromatic face of guanine, respectively (*35*−*37*). Use of these metal-dependent reagents further serves as an important counterpoint to hydroxyl radical mapping of the phosphoribose backbone (*31*). The advantages of NiCR and $CoCl_2$ are made quite evident from their characterization of 5S rRNA from *Xenopus lavis* oocyte (Xlo) as described below.

MATERIALS AND METHODS

Reagents. NiCR [[2,12-dimethyl-3,7,11,17-tetraazacyclo-[11.3.1]heptadeca-1(17),2,11,13,15-pentaenato]nickel(II) perchlorate] was prepared by Dr. James Muller according to published procedures (*38*). Commercially available materials such as $CoCl_2$, $KHSO_5$, and aniline were used without purification. All buffers were made from reagents of the highest available quality and purified water that had been treated with diethyl pyrocarbonate.

Preparation of 5S rRNA. The gene for *X. lavis* oocyte 5S rRNA (*39*) was transcribed in vitro with T7 RNA polymerase as described previously (*40*). The RNA was alternatively labeled at the 5′-terminus by including [γ-^{32}P]-GTP during transcription (*40*) or at the 3′-terminus by T4 RNA ligase in the presence of 5′-[^{32}P]pCp (*41*). RNA samples were purified using a 6% denaturing polyacrylamide gel. Finally, RNA was renatured in Tris-HCl (10 mM, pH 7.0), KCl (25 mM), $MgCl_2$ (0−5 mM), and wheat germ 5S rRNA (2 μg) by heating to 55 °C for 5 min and then cooling under ambient conditions to 20 °C.

Oxidation of Guanine Residues by NiCR and $CoCl_2$. RNA samples (10 nCi ^{32}P label) were incubated with NiCR or $CoCl_2$ (3 μM) in the presence of $KHSO_5$ (100 μM), Tris (10 mM, pH 7), KCl (25 mM), and $MgCl_2$ (0−5 mM) at 20 °C for 30 min. Reactions were quenched by addition of 0.3 M NaOAc, 10 mM EDTA, and 0.5% SDS, extracted with phenol/chloroform, and precipitated with ethanol at −20 °C overnight. The RNA was then treated with 1 M aniline-acetate as described previously (*31*). The fragmentation products were analyzed by denaturing gel (12% polyacrylamide, 7 M urea) electrophoresis and detected by autoradiography.

Alkylation of G Residues. Dimethyl sulfate (DMS) (0.5 μL) was added to renatured RNA (20 μL) and incubated at 20 °C for 5−10 min. The reaction mixture was quenched by β-mercaptoethanol, reduced by $NaBH_4$, and hydrolyzed by aniline-acetate using published conditions (*42*, *43*).

Limited Digestion of Native RNA by T1 RNase. The renatured RNA was treated with RNAse T1 and incubated under ambient conditions for 5 min. Reactions were quenched with 10 M urea and analyzed directly by electrophoresis as described above.

Sequencing Reactions for RNA. Standard sequencing protocols using alkaline conditions and RNases T1 and U2 followed published procedures (*44*, *45*).

RESULTS

Modification of 3′-[^{32}P]-5S rRNA in the Absence of Mg^{2+}. Both NiCR and $CoCl_2$ promoted selective oxidation of guanine in the presence of $KHSO_5$ (Figure 1). Reaction was fully dependent on these metal reagents since no products were observed after incubation with $KHSO_5$ alone (lane 1).

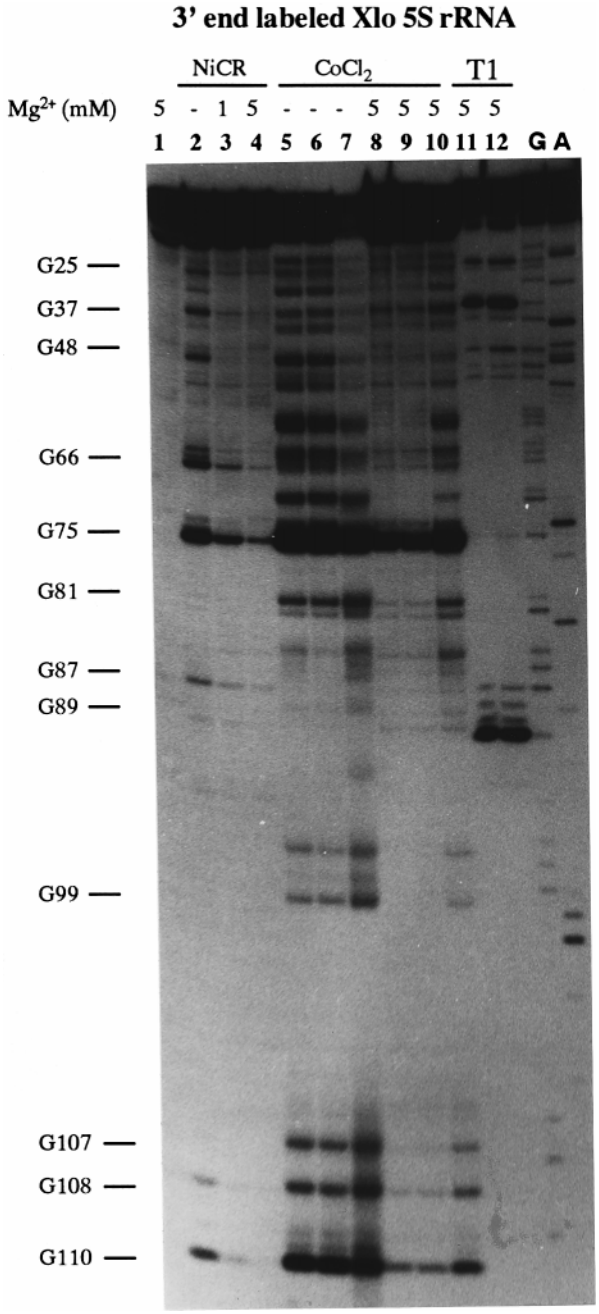

FIGURE 1: Selective modification by NiCR, $CoCl_2$, and RNase T1. 3′-^{32}P-labeled 5S RNA was treated with NiCR (3 μM, lanes 2−4) or $CoCl_2$ (3 μM, lanes 5−10) in the presence of $KHSO_5$ (100 μM, lanes 2−6, 8, and 9; 200 μM, lane 1, 7, and 10) and the indicated concentration of $MgCl_2$ under standard conditions described in Materials and Methods. This RNA was also treated with RNase T1 (0.01 unit, lane 11; 0.05 unit, lane 12) under equivalent conditions. Marker lanes were generated under denaturing conditions by RNase T1 (lane G) and U2 (lane A).

Modification sites were detected throughout this report by diagnostic strand fragmentation induced by aniline-acetic acid (*31*, *43*). This process degrades the oxidized residues and produces 3′-fragments equivalent to those produced by RNase T1. Primer extension may alternatively be used to determine the sites of reaction (*46*), but this procedure was not necessary for 5S rRNA due to its small size.

The extent of guanine oxidation promoted by NiCR had previously been shown to correlate with the environment surrounding guanine N7, and typically residues within an

A-helix are inert (*31*). In the absence of Mg^{2+}, many residues of 5S rRNA such as G25, G37, G48, G64−G66, G75, and G110 were modified by NiCR (lane 2). However, a significant number of residues such as G59−G61, G70, G71, G81, G82, G85, G86, and G97−G99 did not react suggesting that they formed stable helixes under these semi-denaturing conditions.

In contrast to NiCR, $CoCl_2$ promoted oxidation of most all guanine residues in the absence of Mg^{2+} (lanes 5−7). This alternative probe has been used to identify exposure of the aromatic face of guanine and is not generally as sensitive as NiCR to DNA or RNA secondary structure (*37*). However, the dominant sites of modification by NiCR (G48, G66, G75, G108, and G110) were also major sites of modification by $CoCl_2$. In particular, G75 was the most prevalent target of both reactions. At equimolar concentration, $CoCl_2$ typically induces more extensive polynucleotide modification than NiCR, and this was observed for 5S rRNA as well (lane 5 vs lane 2). When the concentration of the terminal oxidant, $KHSO_5$, was doubled in the presence of $CoCl_2$ (lane 7), RNA strands became subject to multiple reactions as evident by the overabundance of small strand fragments.

Modification of 3′-[^{32}P]-5S rRNA in the Presence of Mg^{2+}. 5S rRNA was less susceptible to oxidation upon addition of Mg^{2+} (lane 3 and 4), but the dominant sites of reaction generally remained constant. Since 5 mM Mg^{2+} is sufficient to stabilize the native structure of 5S rRNA (*21*, *47*), modification at residues such as G37, G66, G75, and G87 indicated an unusually high exposure of their N7 positions within the fully folded RNA. G75 remained the major site of reaction under all conditions. A number of residues that were subject to $CoCl_2$-dependent, but not NiCR-dependent, oxidation (G59−G61, G71, G72, and G97−G99) in the absence of Mg^{2+} became inert in the presence of Mg^{2+} (lanes 8 and 9). However, these were again subject to oxidation under more vigorous conditions sustained by a high concentration of $KHSO_5$ (200 μM, lane 10). The presence of Mg^{2+} appeared to inhibit over-reaction of 5S rRNA in this example since the ratio of high- and low-molecular-weight fragments remained constant in the presence of both 100 and 200 μM $KHSO_5$ (lanes 9 and 10).

RNase T1 has frequently been used to characterize 5S rRNA (*20*−*23*), but this enzyme reacts at only a limited number of sites within 5S rRNA. Two of these (G25 and G37) are common targets of NiCR and $CoCl_2$ as well. However, the relative yield of products generated by RNase T1 is very different from those generated by the alternative probes. G89 is most sensitive to RNase T1 and yet only minimally sensitive to NiCR and $CoCl_2$. Conversely, G75 is most sensitive to NiCR and $CoCl_2$ and only minimally sensitive to RNase T1. The basis of these differences is considered in the discussion section below.

Modification of 5′-[^{32}P]-5S rRNA. To examine guanine residues near the 5′ terminus of 5S rRNA, chemical and enzymatic modification was repeated using 5′-labeled RNA. In this case, the RNA fragments produced by metal-dependent oxidation and subsequent aniline-acetic acid treatment are one nucleotide shorter than the corresponding fragments produced by RNase T1, but they migrate more slowly due to formation of a 3′-protonated Schiff base (*30*) (for example, see Figure 2 lanes 4, 7, and G). $CoCl_2$ again promoted modification to a greater extent and at more sites

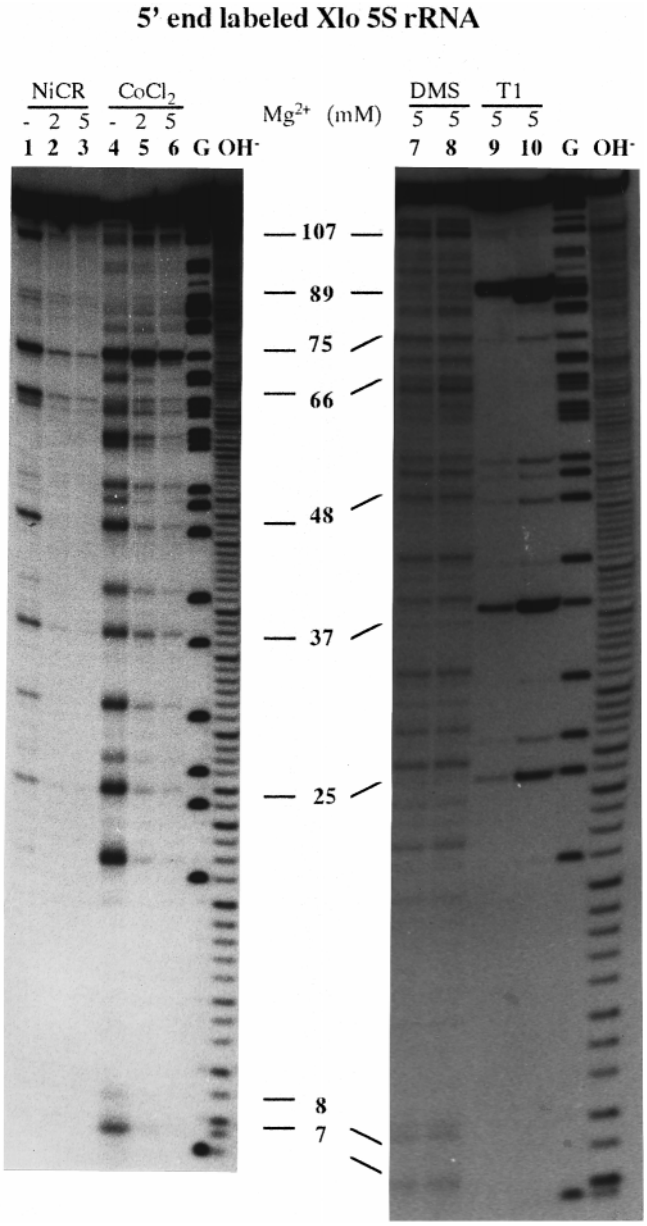

FIGURE 2: Selective modification by NiCR, $CoCl_2$, dimethyl sulfate (DMS), and RNase T1. 5′-^{32}P-labeled 5S RNA was alternatively treated with the indicated reagents in the presence of 0−5 mM $MgCl_2$ under standard conditions described in Materials and Methods. Native RNA samples were treated alternatively with DMS for 5 min (lane 7) and 10 min (lane 8) or RNase T1 (0.01 unit, lane 9; 0.05 unit, lane 10). Marker lanes were generated under denaturing conditions by RNase T1 (lane G) and NaOH (lane OH^-).

than NiCR in both the presence and absence of Mg^{2+}. Since 1 mM Mg^{2+} had only partially suppressed reaction of the 3′-labeled 5S rRNA, the effect of 2 mM Mg^{2+} was examined with the 5′-labeled rRNA. The NiCR-dependent reaction was nearly equivalent in the presence of 2 and 5 mM Mg^{2+} (Figure 2, lanes 2 and 3), whereas the Co^{2+}-dependent reaction was detectably suppressed when the concentration of Mg^{2+} was increased from 2 to 5 mM (Figure 2, lanes 5 and 6). These data suggest that 5S rRNA approaches a native conformation in the presence of 2 mM but not 1 mM Mg^{2+}, and significant unfolding occurs in the absence of Mg^{2+} (Figure 2, lanes 1 and 4).

The dominant sites of reaction in the presence of NiCR, $CoCl_2$, and RNase T1 are revealed equally by 3′- and 5′-

labeled 5S rRNA (Figure 2, lanes 1−6, 9, and 10). The yield of some of the shortest fragments generated from the 5′-labeled RNA might have been the result of over-reaction in the absence of Mg^{2+} (Figure 2, lane 4), but at least G25, G27, G31, and G37 were confirmed as primary sites of reaction by examining the 3′-labeled polynucleotide (Figure 1, lanes 2 and 5). Extensive unfolding of 5S rRNA does not likely result from modification by the metal-dependent probes since they promote guanine oxidation exclusively under these conditions. The more disruptive modification, strand scission, is produced by subsequent incubation with aniline-acetate only after the conformation-specific reaction has been completed. Since RNase T1 promotes direct strand scission during analysis, this probe has a greater potential to generate secondary fragments. However, multiple digestion to form small fragments was not apparent from RNase T1 modification of 5′-labeled 5S rRNA. The ratio of high and low molecular weight products remained constant even after extensive hydrolysis (Figure 2, lanes 9 and 10).

The conformational probes DMS and RNase T1 represent two extremes in structural selectivity. DMS modified almost every guanine in 5S rRNA, as expected for a polymer devoid of tertiary interactions (Figure 2, lanes 7 and 8). Furthermore, the relative uniformity of the DMS reaction is consistent with its insensitivity to variations of secondary structure. In contrast, RNase T1 modified only two major (G37 and G89) and a limited number of minor sites. Without the use of additional reagents such as NiCR and $CoCl_2$, the results of RNase T1 could be ambiguous and misleading. Reaction with this enzyme might solely have reflected guanine accessibility due to lack of base pairing, yet conformational constraints and perturbations associated with enyzme−RNA binding might also have affected target modification.

DISCUSSION

The secondary structure predicted for Xlo 5S rRNA and illustrated in Figure 3 has evolved from considerable phylogenetic analysis (*12*, *13*), chemical modification (*3*, *13*, *20*, *21*), site-directed mutagenesis (*18*, *19*), computer modeling (*10*), and physical characterization (*4*, *11*). Chemical modification alone provided an enormous quantity of data, but its significance is limited by the idiosyncracies of each required reagent. For example, DMS is often too small to act as a sensitive probe for guanine N7, whereas the macromolecule RNase T1 can be too large to access all unpaired guanines (*31*). RNase T1 has the additional potential to induce non-native structures while binding and hydrolyzing the RNA during analysis. Accordingly, the reactive nature of G53 with DMS, a carbodiimide, and RNase T1 (*21*) did not exclude the possibility of base pairing between U28 and G53 in the proposed three-dimensional structure (*10*).

NiCR also appears to bind directly to guanine N7 (*35*, *36*), but this interaction does not seem to affect the conformation of accessible residues (*48*). In addition, this reagent is small enough to gain access to sites that are not available to RNase T1 (*31*). The $CoCl_2$-dependent reaction does not require direct binding to guanine and rather generates sulfate radical, a small, diffusible and anionic oxidant derived from $KHSO_5$, that exhibits an inherent selectivity for guanine (*37*, *49*).

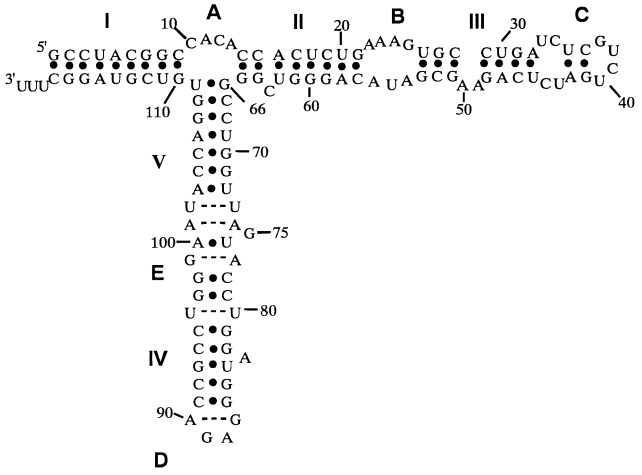

FIGURE 3: Secondary structure of Xlo 5S RNA. Purine-pyrimidine pairing is indicated by (●) and distinguished from purine-purine and pyrimidine-pyrimidine base pairing (- - -).

Helical Regions of 5S rRNA. The general specificity and Mg^{2+} dependence of 5S rRNA oxidation promoted by NiCR and $CoCl_2$ are generally consistent with its formation of helixes I−V and loops A−E (Figure 3). Under native conditions, all guanines within the helical regions, except for a few near loop A (G64−G66, G107, G108, and G110), are stable to NiCR (Figure 4). The unreactive residues within the helixes include those forming noncanonical base pairs such as G8-U111, G60-U18, and G93-U84 (Figure 3). Even G53 loses its reactivity with NiCR as Mg^{2+} is added to stabilize the G53-U26 pairing at the interface of loop B and helix III. Interestingly, residues G27, G51, and G53 within this same region remain subject to weak reaction with RNase T1 (Figure 4). These results may be due to an enzyme-dependent perturbation of 5S rRNA structure similar to that observed previously with a natural sense−antisense complex of *E. coli* (*50*). Alternatively, base stacking in this region may be weak enough to allow sufficient enzyme access. A rather loose stacking or very accessible major groove would also explain the complementary modification promoted by $CoCl_2$. This enhanced reactivity is not likely due to a dynamic unfolding or a low concentration of non-native conformations since they would have been equally detected by NiCR.

Loop E. The designation "loop E" is historic rather than descriptive, since this domain has long been proposed to stack in a distorted helix. The structure of this sequence has received significant attention due to its interesting array of noncanonical base pairing. On the basis of phylogenetic and enzymatic analysis, a helix containing 2 A-G pairs and an extrahelical U was first proposed for loop E (*20*) (Figure 5). However, deletion of the extrahelical U73 yielded an unexpectedly open structure when characterized by NMR (*51*). A second model containing four noncanonical pairs and an extrahelical A77 (Figure 5) was next implicated by a full range of standard chemical probes (*21*). More recently, a third model containing three noncanonical pairs and an extrahelical G75 (Figure 5) was developed from NMR spectroscopy (*11*).

The extraordinary reactivity of G75 with NiCR and $CoCl_2$ in the presence or absence of Mg^{2+} (Figure 4) uniquely supports the latest model specifying G75 as extrahelical. Both

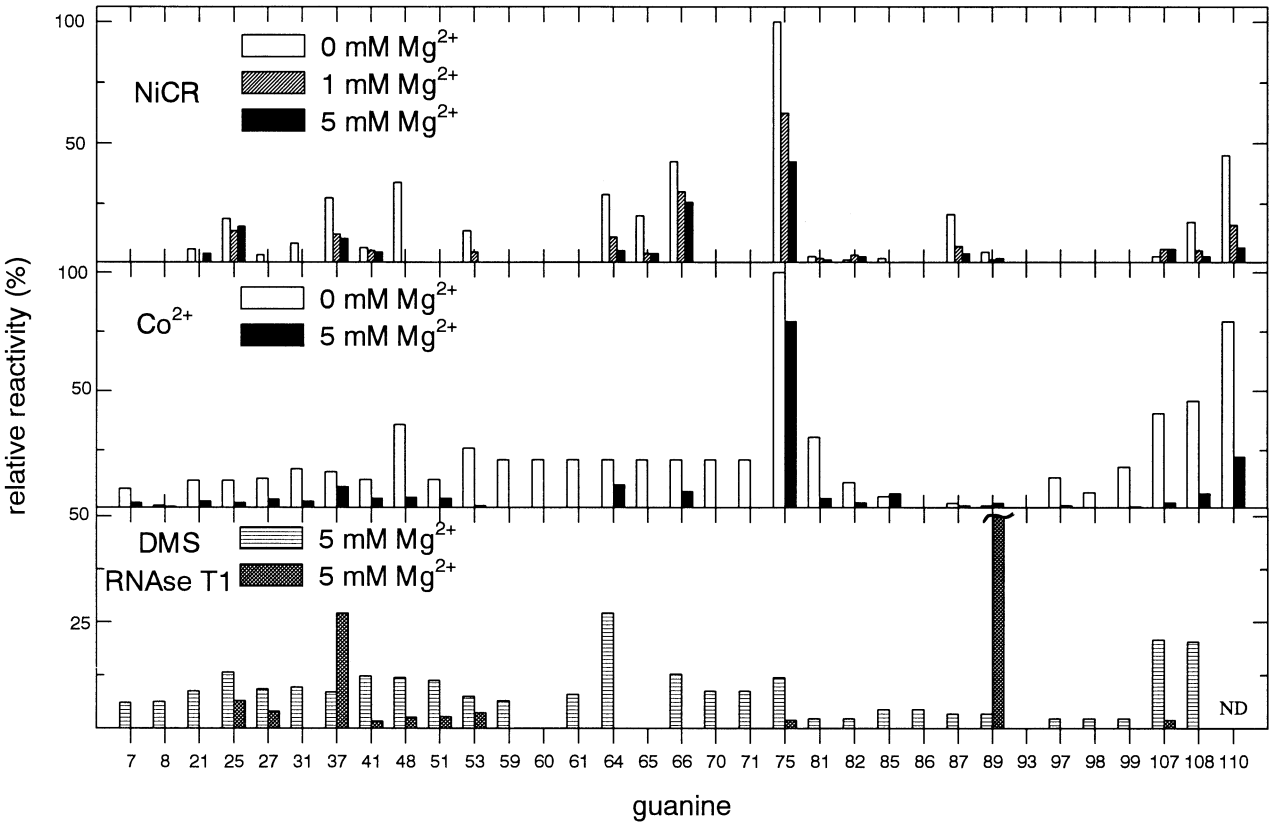

FIGURE 4: Relative reactivity of guanine residues in Xlo 5S RNA. Modification at each site was quantified by densitometric analysis of Figures 1 and 2. The relative reactivity of G89 with RNase T1 extends beyond the indicated range to 100%.

the N7 and aromatic face of this residue are more readily oxidized with these reagents than any other guanine in Xlo 5S rRNA, including those involved in noncanonical base pairs, hairpin loops, and a helical junction. No equivalent hierarchy of modification had previously been detected by other chemical probes. Although G75 is subject to N7 methylation by DMS, the extent of reaction is typical of numerous other guanines in 5S rRNA (Figure 4). In addition, this guanine is only a minor target of RNase T1. This final observation likely signifies a lack of active site binding or recognition rather than a lack of solvent exposure. Together, the observations are consistent with the proposed formation of a base triplet between G75 and the reverse Hoogsteen A100-U76 pair (*11*) that would hold the guanine in the helix with its N7 position accessible to NiCR and cobalt-generated sulfate radical (Figure 5).

The noncanonical structure of loop E is not unique to 5S rRNA, and equivalent structures have been identified in a hairpin ribozyme (*52*) and the sarcin/ricin loop in 28S rRNA (*53*, *54*). Furthermore, the A-G base pair that is common to these domains recurs at other positions within these polynucleotides as well as within other catalytic and ribosomal RNA (*55*−*58*). This unusual pairing appears to be quite stable and well-accommodated by the RNA helix, as indicated by the ability of G99 in loop E to resist modification by NiCR (Figure 4). Protection of guanine may in part derive from an adjacent base triple, but the guanine counterpart in a hairpin ribozyme lacking an apparent base triple is also inert to NiCR (*52*). The structure surrounding the G99-A77 pair in 5S rRNA seems relatively stable even in the absence of Mg^{2+} since only the smallest reagents, DMS and sulfate radical, had access to G99, and no comparable reaction was observed with the more selective NiCR.

Loop D. The tetraloop sequence GAGA of loop D in Xlo 5S rRNA is also common to the sarcin/ricin binding region of 28S rRNA (*53*), and both are thought to form a structure typical of a GNRA loop. Previous characterization of this domain by chemical, computational, and NMR methods (*10*, *54*, *59*, *60*) all describe a hairpin turn that is anchored by a 5′-G···A-3′ base pair and capped by a stack of the central A and G over the 3′-A. Consequently, A88 and A90 stack above and below G89 and shield it from purine oxidation. Although this guanine likely equilibrates among a range of conformations, the exposure of its N7 was expected to be more limited than that of the rigidly held G87 due to a possible hydrogen bond between N7 of G89 and an adjacent ribose hydroxyl group (*60*). Indeed, G87 was modified to a greater extent than G89 in the presence of NiCR under native conditions, and a further enhancement in the reactivity of G87 was observed in the absence of Mg^{2+}. G89 did not exhibit a similar increase in reactivity, and therefore a general unfolding of the loop is not likely. Such an unfolding is also not consistent with the lack of significant $CoCl_2$-dependent modification of G87 and G89 in the absence of Mg^{2+}. Interestingly, G89 rather than G87, G75, or any other guanine was the single most prevalent target of RNase T1 (Figure 4) (*21*, *61*). Dominant modification at this site is inconsistent with all of the possible variants of GNRA tetraloop structure (*10*, *54*, *59*, *60*). Perhaps RNase T1 preferentially binds and stabilizes a minor perturbation of the native structure for which the purine of G89 has rotated into solution to facilitate association with the enzyme.

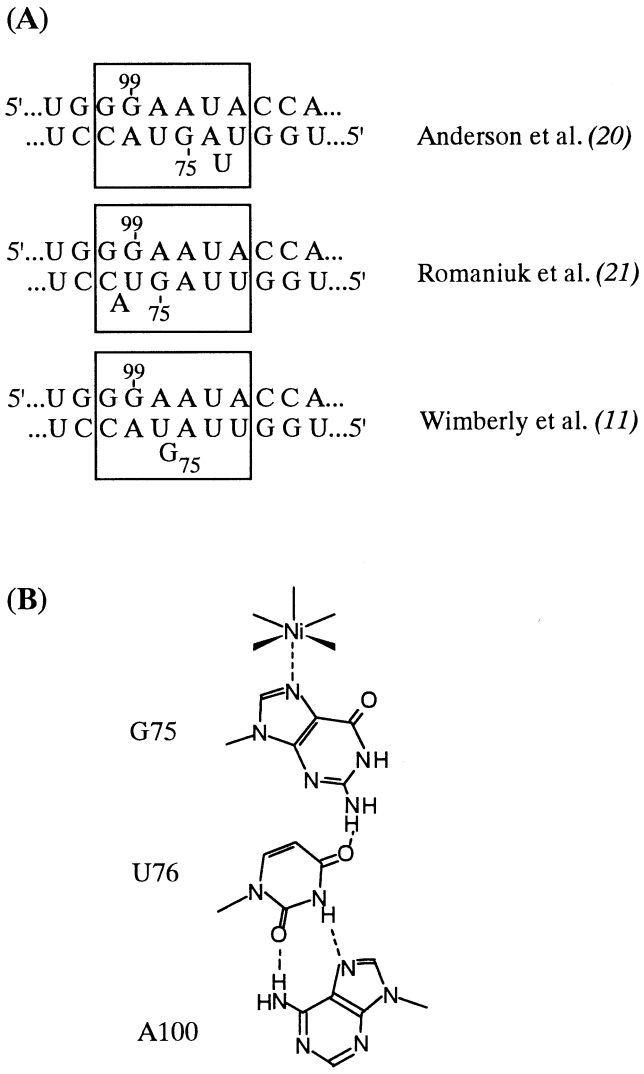

FIGURE 5: (A) Alternative structures proposed for loop E. (B) Possible interactions between the nickel complex, G75, U76, and A100 (adapted from ref 11).

Loops B and C. The internal and hairpin loops B and C are stabilized by numerous stacking interactions but few base pairs (*10*). Accordingly, these structures may be readily denatured under mild conditions, and the extent of modification likely depends on the tendencies of each base to adopt an extrahelical versus stacked conformation. In the absence of Mg^{2+}, most guanines and especially G25, G37, and G48 of loops B and C and helix III were modified by NiCR. Even in the presence of Mg^{2+}, G25 and G37 likely equilibrated between a variety of unpaired conformations and persisted as moderate targets of all reagents examined, NiCR, $CoCl_2$, DMS, and RNase T1. Base pairing of G41-C36 and G53-U26 limited the reactivity of these guanines in the absence of $Mg^{2+}$and further suppressed their reactivity in the presence of 5 mM Mg^{2+}. Generally, few guanines in these domains are completely protected from modification, but NiCR was most selective and thus most useful for distinguishing the accessibility of these residues.

Loop A. The conformation of loop A continues to pose some of the most challenging and interesting questions concerning 5S rRNA structure and function. This loop forms the junction of helixes I, II, and V, and consequently it sets the relative orientation of all three helical extensions. This

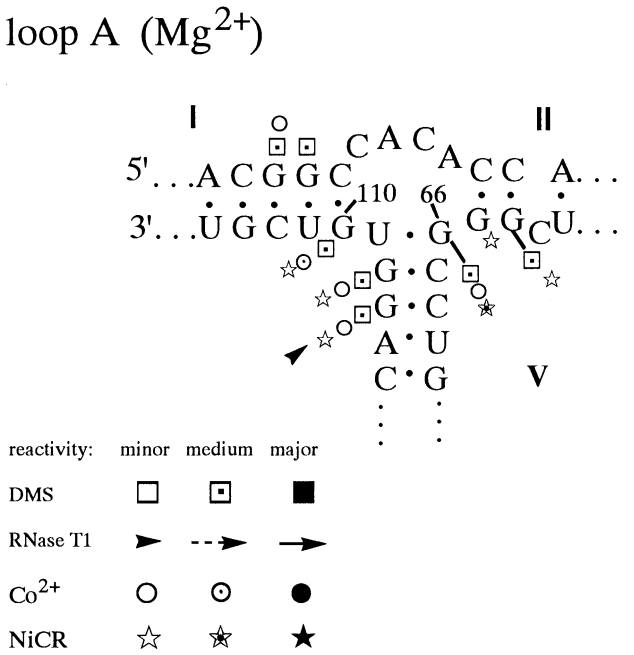

FIGURE 6: Relative reactivity of guanine residues in the vicinity of loop A.

in turn strongly affects 5S rRNA recognition by TFIIIa (*61*−*63*). Chemical, genetic, and computational analysis of this region has suggested that helixes II and V are nearly collinear for the Xlo and *E. coli* sequences (*10*, *23*, *62*, *64*). However, helixes I and V appear colinear in 5S rRNA from *Sulfolobus acidocaldarius* (*27*). Interconversion of these forms may be facile and essential for biological function (*4*, *25*, *65*).

The inability of RNase T1 to modify loop A extensively (Figure 6) is consistent with previous investigations (*20*, *21*, *61*, *63*) and supports a structural model for which all of the guanine residues participate in base pairing (*10*). Modification of guanine N7 by DMS is somewhat more extensive in the vicinity of loop A than in other regions of 5S rRNA (Figure 4), but these data do not preclude base pairing. Extensive mutagenesis of loop A has confirmed C9-G110, C14-G65, and G66-U109 pairing and also indicated hydrogen bonding between A13 and G66 (*62*). In addition, these studies illustrated the plasticity of loop A by identifying deletion mutants with alternative base pairing arrangements within this region. Only this last result might have been used to anticipate facile modification of loop A by NiCR and $CoCl_2$.

Guanine residues 64−66, 107, 108, and 110 were among the most reactive targets of NiCR under denaturing (−Mg^{2+}) and native (+Mg^{2+}) conditions, and all border loop A. This reactivity is not easily dismissed as merely a result of electrostatic attraction and binding of the cationic nickel reagent to the highly anionic junction of three helixes. Sulfate radical, the anionic oxidant generated by $CoCl_2$, produced a similar profile of modification (Figures 4 and 6). Furthermore, modification of G107, G108, and G110 near the 3′ terminus of 5S rRNA was not likely a consequence of over-reaction since modification of this region was evident using both 3′- and 5′-labeled rRNA.

Oxidation of loop A by NiCR is perhaps diagnostic of a series of dynamic structures or a single structure that is more accessible than previously indicated by the three-dimensional

model (*10*). The existence of multiple conformations is compatible with the apparent flexibility of this loop (*4*) and the alternative base pairing of loop A deletion mutants (62). However, only minor changes to the static model of Xlo 5S rRNA are necessary to explain guanine reaction with NiCR. The current model already predicts the necessary exposure of G110, since its N7 is not protected by stacking interactions. Only the orientation of the G66-U109 base pair would require some shifting in order to expose its N7 position in accord with its reactivity. Modification at this site is second only to that of the extrahelical G75 of loop E. Finally, the limited reaction of G107 and G108 could be resolved by minimal unwinding of helix V. Such changes in the model are supported in part by the general reliability that NiCR has demonstrated for other regions of 5S rRNA and other RNA structures in general (*31*, *50*, *52*, *65*, *66*).

Conclusion. The complementary reagents, NiCR and $CoCl_2$, provided significant advantages over the common alternatives, DMS and RNase T1, for determining the accessibility of guanine. DMS is too small to detect secondary structure, and RNase T1 is often too large to approach guanine residues that would otherwise be recognized as substrates. The nickel and cobalt reagents alternatively generate metal-bound and diffusible oxidants with a balance of size and specificity (*35*, *37*). NiCR was the first reagent to confirm the extrahelical orientation of G75 within loop E as suggested by previous NMR model studies (*11*) and the first to modify G87 and G89 of loop D in reasonable accord with their proposed range of comformations (*10*, *54*, *60*). This reagent also provided new data for refining the flexibility and organization of loop A and its adjacent helixes.

ACKNOWLEDGMENT

We thank J. Muller for NiCR, D. Bogenhagen for the clone of Xlo 5S RNA, and both for their expertise and helpful discussions.

REFERENCES

1. White, S. A., Nilges, M., Huang, A., Brünger, T., and Moore, P. B. (1992) *Biochemistry 31*, 1610−1621.
2. Nazar, R. N. (1991) *J. Biol. Chem. 266*, 4562−4567.
3. Chow, C. S., Hartmann, K. M., Rawlings, S. L., Huber, P. W., and Barton, J. K. (1992) *Biochemistry 31*, 3534−3542.
4. Hagerman, P. J. (1997) *Annu. Rev. Biophys. Biomol. Struct. 26*, 139−156.
5. Huber, P. W., and Wool, I. G. (1984) *Proc. Natl. Acad. Sci. U.S.A. 81*, 322−326.
6. Dokudovskaya, S., Dontsova, O., Shpanchenko, O., Bogdanov, A., and Brimacombe, R. (1996) *RNA 2*, 146−152.
7. Green, R., and Noller, H. F. (1997) *Annu. Rev. Biochem. 66*, 679−716.
8. Picard, B., and Wegnez, M. (1979) *Proc. Natl. Acad. Sci. U.S.A. 76*, 241−245.
9. Pelham, H. R. B., and Brown, D. D. (1980) *Proc. Natl. Acad. Sci. U.S.A. 77*, 4170−4174.
10. Westhof, E., Romby, P., Romaniuk, P. J., Ebel, J.-P., Ehresmann, C., and Ehresmann, B. (1989) *J. Mol. Biol. 207*, 417−431.
11. Wimberly, B., Varani, G., and Tinoco, I. (1993) *Biochemistry 32*, 1078−1087.
12. Fox, G. E., and Woese, C. R. (1975) *Nature 256*, 505−507.
13. Delihas, N., Andersen, J., and Singhal, R. P. (1984) *Prog. Nucleic Acid Res. Mol. Biol. 31*, 161−188.
14. Böhm, S., Fabian, H., Venyaminov, S. Y., Matveev, S. V., Lucius, H., Welfle, H., and Filimonov, V. V. (1981) *FEBS Lett. 132*, 357−361.
15. Hancock, J., and Wagner, R. (1982) *Nucleic Acids Res. 10*, 1257−1269.
16. Pieler, T., and Erdmann, V. A. (1982) *Proc. Natl. Acad. Sci. U.S.A. 79*, 4599−4603.
17. Göringer, H. U., and Wagner, R. (1986) *Nucleic Acids Res. 14*, 7473−7485.
18. Leal de Stevenson, I., Romby, P., Baudin, F., Brunel, C., Westhof, E., Ehresmann, C., Ehresmann, B., and Romaniuk, P. J. (1991) *J. Mol. Biol. 219*, 243−255.
19. Brunel, C., Romby, P., Westhof, E., Romaniuk, P. J., Ehresmann, B., and Ehresmann, C. (1990) *J. Mol. Biol. 215*, 103−111.
20. Anderson, J., Delihas, N., Hanas, J. S., and Wu, C.-W. (1984) *Biochemistry 23*, 5759−5766.
21. Romaniuk, P. J., Leal de Stevenson, I., Ehresmann, C., Romby, P., and Ehresmann, B. (1988) *Nucleic Acids Res. 16*, 2295−2312.
22. Romby, P., Westhof, E., Toukifimpa, R., Mache, R., Ebel, J.-P., Ehresmann, C., and Ehresmann, B. (1988) *Biochemistry 27*, 4721−4730.
23. Brunel, C., Romby, P., Westhof, E., Ehresmann, C., and Ehresmann, B. (1991) *J. Mol. Biol. 221*, 293−308.
24. Correll, C. C., Freeborn, B., Moore, P. B., and Steitz, T. A. (1997) *Cell 91*, 705−712.
25. Kao, T. H., and Crothers, D. M. (1980) *Proc. Natl. Acad. Sci. U.S.A. 77*, 3360−3364.
26. Kime, M. J., and Moore, P. B. (1982) *Nucleic Acids Res. 10*, 4973−4983.
27. Shen, Z., and Hagerman, P. J. (1994) *J. Mol. Biol. 241*, 415−430.
28. Chastain, M., and Tinoco, I. (1991) *Prog. Nucleic Acid Res. Mol. Biol. 41*, 131−177.
29. Westhof, E., Masquida, B., and Jaeger, L. (1996) *Folding Des. 1*, R78−R88.
30. Ehresmann, C., Baudin, F., Mougel, M., Romby, P., Ebel, J.-P., and Ehresmann, B. (1987) *Nucleic Acids Res. 15*, 9109−9129.
31. Chen, X., Woodson, S. A., Burrows, C. J., Rokita, S. E. (1993) *Biochemistry 32*, 7610−7616.
32. Heinemann, U., and Saenger, W. (1985) *Pure Appl. Chem. 57*, 417−422.
33. Conway, L., and Wickens, M. (1989) *Methods Enzymol. 180*, 369−377.
34. Chanfreau, G., and Jacquier, A. (1996) *EMBO J. 15*, 3466−3476.
35. Burrows, C. J., Rokita, S. E. (1994) *Acc. Chem. Res. 27*, 295−301.
36. Burrows, C. J., and Rokita, S. E. (1995) in *Metal Ions in Biological Systems* (Sigel, H., Ed.) pp 537−560, Marcel Dekker, New York.
37. Muller, J. G., Zheng, P., Rokita, S. E., Burrows, C. J. (1996) *J. Am. Chem. Soc. 118*, 2320−2325.
38. Karn, J. L., and Busch, D. H. (1966) *Nature 211*, 160−162.
39. Bogenhagen, D. F. (1993) *Mol. Cell. Biol. 13*, 5149−5158.
40. Sands, M. S., and Bogenhagen, D. F. (1991) *Nucleic Acids Res. 19*, 1791−1796.
41. England, T. E., Bruce, A. G., and Uhlenbeck, O. C. (1980) *Methods Enzymol. 65*, 65−74.
42. Peattie, D. A. (1979) *Proc. Natl. Acad. Sci. U.S.A. 76*, 1760−1764.
43. Peattie, D. A., and Gilbert, W. (1980) *Proc. Natl. Acad. Sci. U.S.A. 77*, 4679−4682.
44. Donis-Keller, H., Maxam, A. M., and Gilbert, W. (1977) *Nucleic Acids Res. 4*, 2527−2538.
45. Donis-Keller, H. (1980) *Nucleic Acids Res. 8*, 3133−3142.
46. Woodson, S. A., Muller, J. G., Burrows, C. J., and Rokita, S. E. (1993) *Nucleic Acids Res. 21*, 5524−5525.
47. Leontis, N. B., Ghosh, R., Moore, P. B. (1986) *Biochemistry 25*, 7386−7392.
48. Shih, H.-C., Tang, N., Burrows, C. J., and Rokita, S. E. (1998) *J. Am. Chem. Soc.* (submitted).
49. Neta, P., Huie, R. E., and Ross, A. B. (1988) *J. Phys. Chem. Ref. Data 17*, 1027−1247.

50. Schmidt, M., Zheng, P., and Delihas, N. (1995) *Biochemistry 34*, 3621−3631.
51. Varani, G., Wimberly, B., and Tinoco, I. (1989) *Biochemistry 28*, 7760−7772.
52. Butcher, S. E., and Burke, J. M. (1994) *J. Mol. Biol. 244*, 52−63.
53. Moazed, D., Robertson, J. M., and Noller, H. F. (1988) *Nature 334*, 362−364.
54. Szewczak, A. A., and Moore, P. B. (1995) *J. Mol. Biol. 247*, 81−98.
55. Gautheret, D., Konings, D., and Gutell, R. R. (1994) *J. Mol. Biol. 242*, 1−8.
56. Pley, H. W., Flaherty, K. M., and McKay, D. B. (1994) *Nature 372*, 68−74.
57. Cia, Z., and Tinoco, I. (1996) *Biochemistry 35*, 6026−6036.
58. Sowkowski, A., Shippy, R., and Hampel, A. (1997) *Biochemistry 36*, 3930−3940.
59. Heus, H. A., and Pardi, A. (1991) *Science 253*, 191−194.
60. Jucker, F. M., Heus, H. A., Yip, P. F., Moors, E. H. M., and Pardi, A. (1996) *J. Mol. Biol. 264*, 968−980.
61. Christiansen, J., Brown, R. S., Sproat, B. S., and Garrett, R. A. (1987) *EMBO J. 6*, 453−460.
62. Baudin, F., Romaniuk, P. J., Romby, P., Brunel, C., Westhof, E., Ehresmann, B., and Ehresmann C. (1991) *J. Mol. Biol. 218*, 69−81.
63. McBryant, S. J., Veldhoen, N., Gedulin, B., Leresche, A., Foster, M. P., Wright, P. E., Romaniuk, P. J., and Gottesfeld, J. M. (1995) *J. Mol. Biol. 248*, 44−57.
64. Christensen, A., Mathiesen, M., Peattie, D., and Garrett, R. A. (1985) *Biochemistry 24*, 2284−2291.
65. Li, H., Dalal, S., Kohler, J., Vilardell, J., and White, S. A. (1995) *J. Mol. Biol. 250*, 447−459.
66. Chen, X., Chamorro, M., Lee, S. I., Shen, L. X., Hines, J. V., Tinoco, I., and Varmus, H. E. (1995) *EMBO J. 14*, 842−852.

BI972480L